An Uncertainty Estimation Exercise with the Finite-Difference and Finite-Volume Versions of PARNASSOS

Luís Eça and Martin Hoekstra

Abstract

This paper presents the applications of the finite-difference and finite-volume versions of PARNASSOS to the five grid sets available for the Workshop on CFD Uncertainty Analysis. The one-equation model proposed by Menter has been applied with the finite-difference code whereas the Spalart & Allmaras model has been applied with the two versions.

Uncertainty estimations have been performed for the selected flow quantities using a least squares root version of the Grid Convergence Index method.

A wide range of observed orders of accuracy is obtained and there are several situations where it is difficult to classify the convergence condition. Therefore, the application of the present procedure to practical calculations still requires some experience and careful interpretation to obtain a reliable uncertainty estimation based on Richardson extrapolation.

1 Introduction

Model testing is still the most used and widely accepted approach in ship hydrodynamic investigations, but there is no doubt that the role of Computational Fluid Dynamics (CFD) in design problems is growing. But where it is standard practice in experimental fluid dynamics to indicate the uncertainty of a specific measurement, it is hard to believe that CFD may establish itself as a reliable alternative and complement to model testing without indicating the numerical uncertainty of a given prediction.

In recent years, we have made several attempts to establish uncertainty estimations of numerical calculations of incompressible turbulent flows. These attempts were based on grid refinement studies and the Grid Convergence Index, GCI, proposed by Roache, [1]. We found that the estimation of the numerical uncertainty of a complex turbulent flow computation can be cumbersome. This has led us to compute a wide variety of flows, ranging from simple 2-D turbulent boundary-layers, [2], to ship stern flows at full scale Reynolds numbers, [3], and to estimate the discretisation errors.

The outcome of our previous work is an uncertainty estimation procedure based on a least squares version of the GCI method, [4]. This procedure incorporates the experience collected from the different test cases computed, but it still requires thorough testing to evaluate its applicability to practical engineering applications, which often involve a complex turbulent flow.

In [4], we have given an overview of the results obtained for the two test cases selected for the Workshop on CFD Uncertainty Analysis, [5], using the finite-difference version of PARNASSOS, [6], and several eddy-viscosity turbulence models. In the present paper, we present the results obtained in the same test cases using two alternative discretizations in PARNASSOS: a finite-difference approach applied to a weak formulation of the continuity and momentum equations and a finite volume technique applied to the strong conservation form of the equations, [7]. Both versions find a coupled solution of the continuity and momentum equations using the continuity equation in its original form. For the present exercise, we have only considered two one-equation turbulence models: the Spalart & Allmaras model, [8] and the model proposed by Menter in [9].

The paper is organized in the following way: the next section gives an overview of the two versions of PARNASSOS and describes the boundary conditions applied in both test cases; for the sake of completeness, section 3 presents the uncertainty estimation procedure; the results are presented and discussed in section 4 and the conclusions are summarized in section 5.

2 PARNASSOS

The 2-D versions of PARNASSOS solve the steady, incompressible, Reynolds-averaged Navier Stokes equations using eddy-viscosity turbulence models. Details of the implementation of the two versions are given in [6] and [7]. The main properties of the two versions are summarized below.

- The finite-difference, FD, version discretizes the continuity and momentum equations written in Contravariant form, which is a weak conservation form. The finite-volume, FV, version discretizes the strong conservation form of the equations.

- The FD version computes the momentum balance along the directions of the curvilinear coordinate system, whereas the FV version calculates the momentum balance for its Cartesian components.

- The FD code has a fully-collocated arrangement with the unknowns and the discretization centered at the grid nodes. In the FV code unknowns are defined at the centre of each cell.

- Both versions apply Newton linearization to the convective terms and are at least second order accurate for all the terms of the continuity and momentum equations. Third-order upwind discretisation is applied to the convective terms.

- The linear system of equations formed by the discretized continuity and momentum equations is in both versions solved simultaneously with GMRES, [10], using a coupled ILU preconditioning.

- Under-relaxation is applied with a quasi time-derivative term.

- The transport equations for the turbulence quantities are discretized with first-order upwind schemes in the FD version. The FV method on the other hand adopts second order discretization. However, flux limiters have to be applied in the interpolations at the cell faces to avoid the appearance of negative turbulence quantities.

- The linearization procedure of the production and dissipation terms of the turbulence quantities follows the standard approach, i.e. production is added to the right-hand side and dissipation to the main-diagonal.

- The solution of the turbulence quantities transport equations is uncoupled from solving the continuity and momentum equations.

2.1 Boundary Conditions

The computational domains of the two test cases have some common features: a vertical inlet boundary, two solid walls and a vertical outlet boundary.

2.1.1 Inlet boundary

At the inlet boundary U^1, U^2 and the turbulent quantities are specified from the input data generated for the Workshop.

The pressure is extrapolated from the interior of the domain, assuming that its second derivative in the streamwise direction is zero.

2.1.2 Solid walls

At the walls, the no-slip and impermeability conditions are applied, which leads to $U^1 = U^2 = 0$. The unknowns of the two selected eddy-viscosity turbulence models are proportional to the eddy-viscosity and so their value at the wall is also 0.

In the FD version of the method, the momentum equation in the normal direction is solved at the wall to obtain the pressure value; in the FV version the pressure at the wall is found from extrapolation from the interior of the domain.

2.1.3 Outlet boundary

U^1, U^2 and the turbulence quantities are extrapolated from the interior of the domain. For the two velocity components a linear extrapolation is performed, whereas for the turbulence quantities we have assumed that the first derivative in the streamwise direction is zero. The pressure is set to zero.

3 UNCERTAINTY ESTIMATION PROCEDURE

A detailed description of the present procedure is given in [4]. Therefore, we will only present its main features in this section.

The basis of our procedure for the estimation of the uncertainty U of the solution on a given grid is the standard Grid Convergence Index (GCI) method, [1], which says

$$U = F_s |\delta_{RE}| \, . \tag{1}$$

F_s is a safety factor and δ_{RE} is the error estimation[1] obtained by Richardson extrapolation:

[1] We are considering here the discretization error. Of course there are also round-off errors and iterative errors but they are assumed in this section to be negligible.

$$\delta_{RE} = \phi_i - \phi_o = \alpha h_i^p \,, \tag{2}$$

where ϕ_i is the numerical solution of any local or integral scalar quantity on a given grid (designated by the subscript $_i$), ϕ_o is the estimated exact solution, α is a constant, h_i is a parameter which identifies the representative grid cell size and p is the observed order of accuracy.

ϕ_o, α and p are computed with a least squares root approach that minimizes the function:

$$S(\phi_o, \alpha, p) = \sqrt{\sum_{i=1}^{n_g} \left(\phi_i - (\phi_o + \alpha h_i^p)\right)^2} \,, \tag{3}$$

where n_g is the number of grids available. The minimum of (3) is found by setting the derivatives of $S(\phi_o, \alpha, p)$ with respect to ϕ_o, p_j and α_j equal to zero, [3].

The apparent convergence condition is then decided as follows:

1. $p > 0$ for $\phi \Rightarrow$ Monotonic convergence.
2. $p < 0$ for $\phi \Rightarrow$ Monotonic divergence.
3. $p^* < 0$ for $\phi_i^* = |\phi_{i+1} - \phi_i| \Rightarrow$ Oscillatory divergence.
4. Otherwise $\Rightarrow$ Oscillatory convergence.

When the observed order of accuracy is larger than 2, we assume the representation of the error estimation to be given by :

$$\delta_{RE2} = \phi_i - \phi_o = \alpha_1 h_i^2 + \alpha_2 h_i^3 \,, \tag{4}$$

which is also solved in the least squares root sense minimizing the function:

$$S(\phi_o, \alpha_1, \alpha_2) = \sqrt{\sum_{i=1}^{n_g} \left(\phi_i - (\phi_o + \alpha_1 h_i^2 + \alpha_2 h_i^3)\right)^2} \tag{5}$$

In the cases of monotonic convergence, the standard deviation of the fit, U_s, is used as one of the contributions of the uncertainty. U_s is given by

$$U_s = \sqrt{\frac{\sum_{i=1}^{n_g} \left(\phi_i - (\phi_o + \alpha h_i^p)\right)^2}{n_g - 3}} \quad \text{or} \quad U_s = \sqrt{\frac{\sum_{i=1}^{n_g} \left(\phi_i - (\phi_o + \alpha_1 h_i^2 + \alpha_2 h_i^3)\right)^2}{n_g - 3}} \,. \tag{6}$$

We can summarize our procedure for the estimation of the numerical uncertainty, valid for a nominally second-order accurate method, as follows:

1. The observed order of accuracy is estimated with the least squares root technique to identify the apparent convergence condition according to the definition given above.
2. For monotonic convergence with $0.5 < p \leq 2$:

   The uncertainty is estimated with the G.C.I., equation (1), using $F_s = 1.25$ and the numerical error estimated with Richardson extrapolation, equation (2), using the least squares root technique. The standard deviation of the fit, U_s, equation (6), is added to the uncertainty.

3. For monotonic convergence with $2 < p \leq 3$:

   The uncertainty is estimated with the G.C.I., equation (1), using

   $$U = 1.25\max(|\delta_{RE}|, |\delta_{RE2}|) \; .$$

   The standard deviation of the fit, U_s, equation (6), is added to the uncertainty.

4. For monotonic convergence with $p \leq 0.5$ or $p > 3$ and for oscillatory convergence :

   U is set equal to the maximum difference between the solutions obtained in the available grids[2] multiplied by a factor of safety, $F_s = 3$.

5. The uncertainty estimation fails for the two divergence conditions.

In the present exercise, we have estimated an uncertainty estimation even when apparent divergence is determined. The maximum difference between all the results available is multiplied by 3 to obtain this estimate.

4 Results

In this paper we will restrict ourselves to the flow quantities selected for the Workshop, namely:

- The friction resistance coefficient of the bottom wall, $(C_F)_b$.
- The friction resistance coefficient of the top wall, $(C_F)_t$.
- The pressure resistance coefficient of the bottom wall, $(C_P)_b$.
- The separation point for the flow over the hill, x_{sep}/h.
- The re-attachment point on the bottom wall, x_{ret}/h.
- The two Cartesian components of the velocity, U^1 and U^2, the pressure coefficient, C_p, and the eddy-viscosity, ν_t, at the three selected locations for the three flows.

The uncertainty of any flow variable will be designated by U and the observed order of accuracy by p. In the finite-difference version we have performed calculations with the two one-equation turbulence models, whereas for the finite volume version we have used only the Spalart & Allmaras turbulence model.

The numerical results of all these calculations are included in the collected information of the Workshop, [5]. Therefore, we will focus mainly on the convergence of the numerical solutions with the grid refinement.

[2] In this case the 4 finest grids available are used to obtain an estimate of the error.

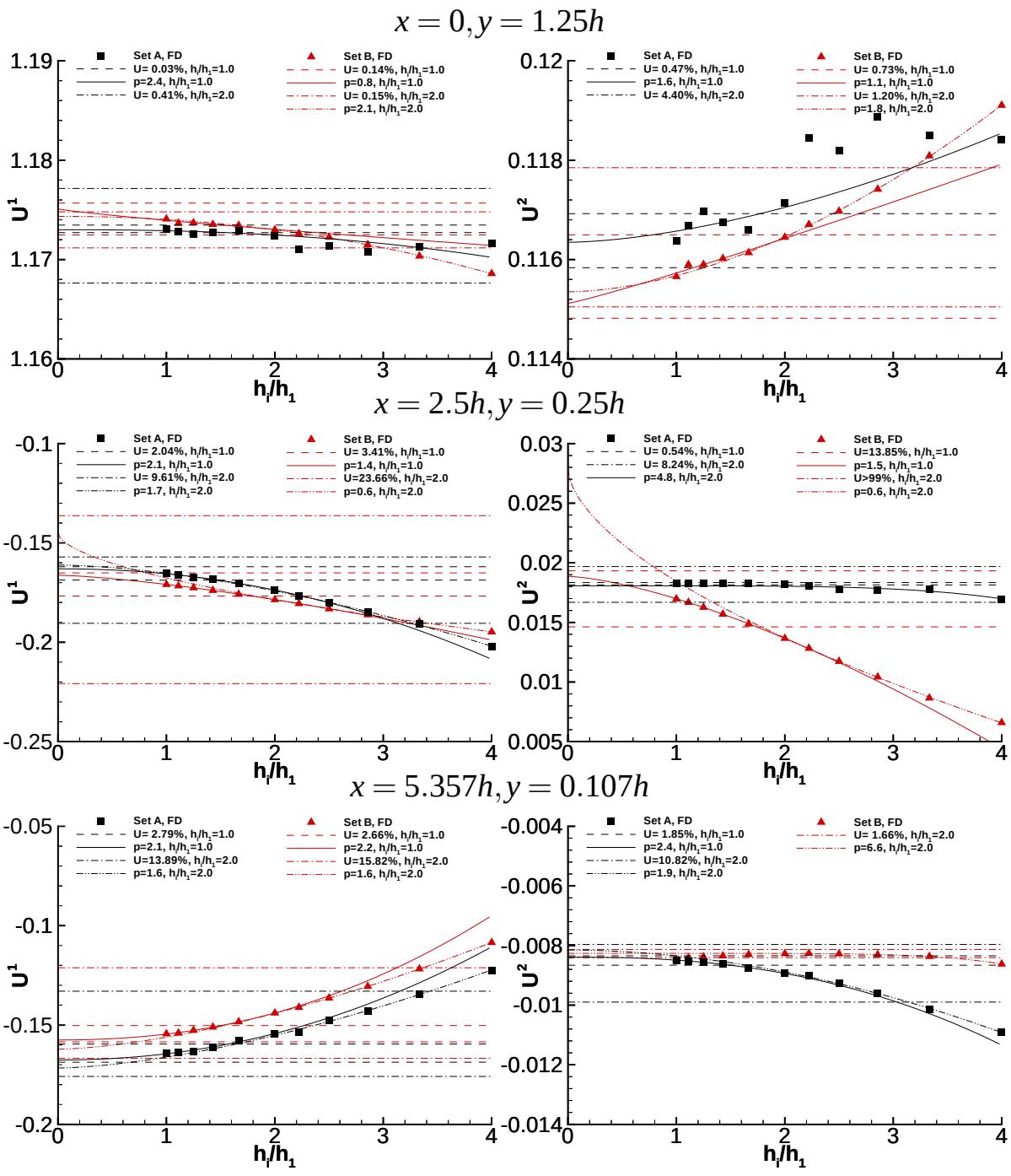

Figure 1: Convergence with the grid refinement of local flow quantities. Flow over a 2-D hill calculated with Menter's one-equation model.

4.1 Flow over a hill, case C-18

For this test case we have computed the solution for the 11 grids of the two grids sets using the FD code. With the FV version, the finest grid computed includes only 281×281 grid nodes. Three

uncertainty estimates were performed for each grid set:

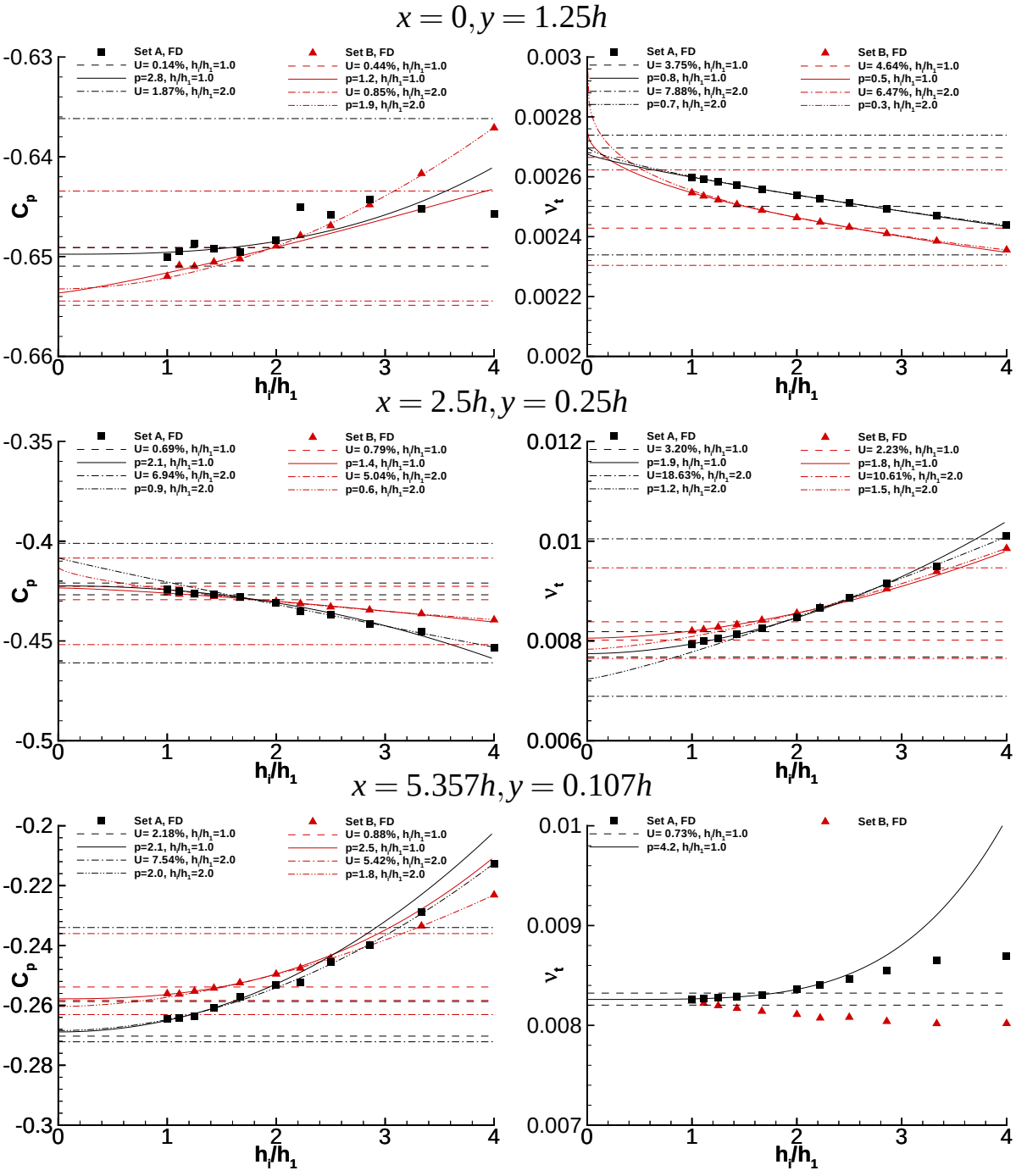

Figure 1: (Cont.) Convergence with the grid refinement of local flow quantities. Flow over a 2-D hill calculated with Menter's one-equation model.

1. The uncertainty of the FD finest grid solution, $h_i/h_1 = 1$, using six grids covering a grid refinement ratio of 2.

2. The uncertainty of the FD solution in the 201×201 grid, $h_i/h_1 = 2$, using six grids covering a grid refinement ratio of 2.

3. The uncertainty of the FV solution in the 281×281 grid, $h_i/h_1 = 1.4$, using six grids covering a grid refinement ratio of 2.

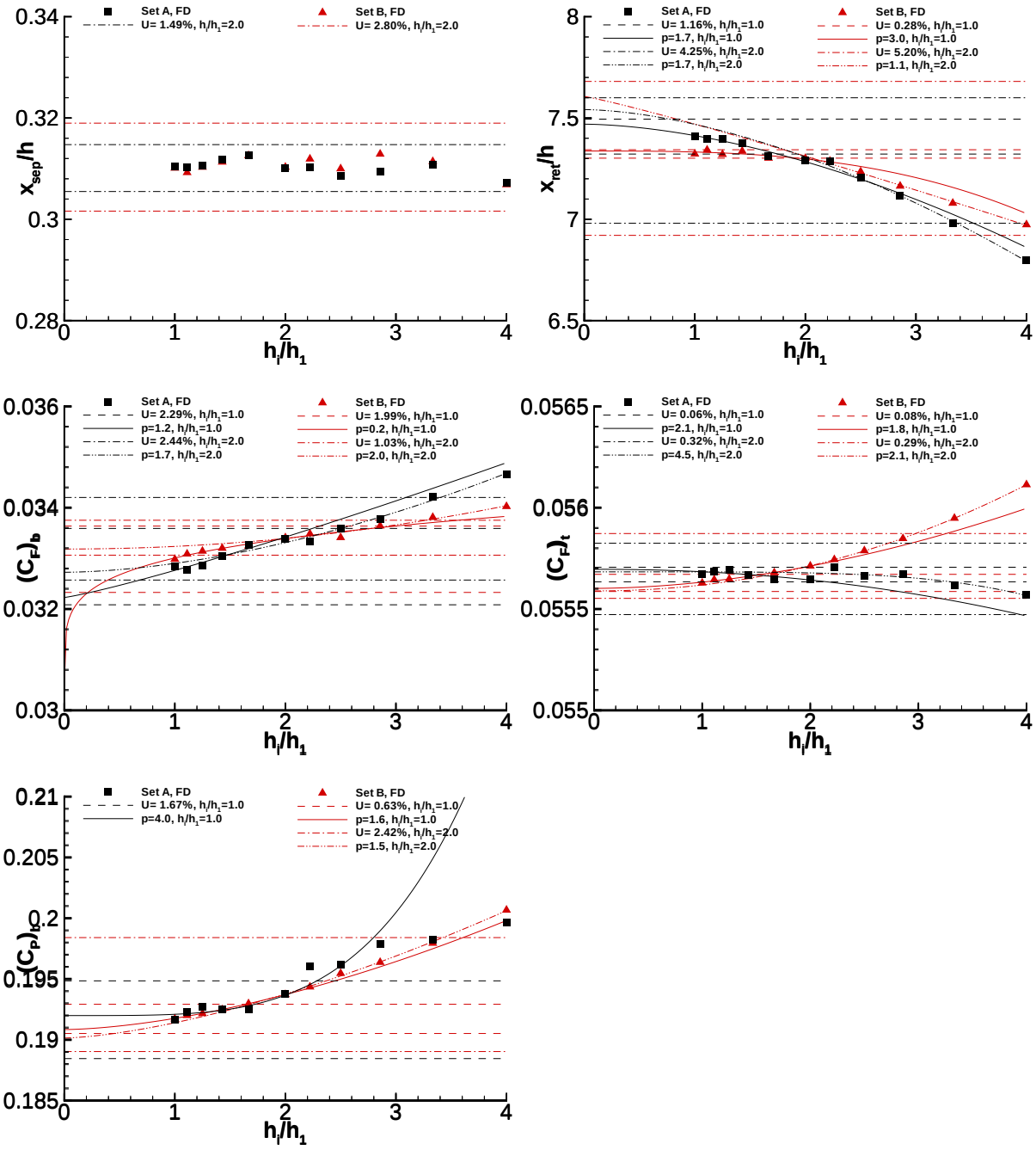

Figure 2: Convergence with the grid refinement of separation and re-attachment points and resistance coefficients. Flow over a 2-D hill calculated with Menter's one-equation model.

4.1.1 Menter's model

Figure 1 presents the convergence of the local flow quantities with the grid refinement at the three selected locations. The data plotted suggest the following remarks:

- The amount of scatter in the data depends on the grid set, the flow quantity and the location selected.
- As one would expect, the uncertainty estimated for the $h_i/h_1 = 2$ grid is larger than the one obtained for the finest grid solution.
- There is overlap between all the error bars estimated for each case. However, the observed order of accuracy exhibits a wide range of values and there are several cases with non-monotonic convergence.
- The results obtained for ν_t at $x = 5.357h, y = 0.107h$ show how difficult the application of an "automatic procedure" for uncertainty estimation based on grid refinement studies is. The results of grid set B lead to apparent divergence in the two grids tested...

These results are consistent with our previous experience and seem to indicate that one of the main difficulties of this type of procedure is the classification of the apparent convergence or divergence condition.

The convergence of the location of the separation and re-attachment points with the grid refinement is illustrated in figure 2. The three resistance coefficients are also depicted in figure 2 as a function of the grid density.

The determination of the separation point does not exhibit a strong dependence on the grid refinement level, but the convergence behaviour is not monotonic. It is frustrating to obtain apparent oscillatory convergence for the coarsest grids of both sets, whereas the data of the six finest grids lead to apparent divergence.

The usual trend is observed that the integral quantities in general present more consistent uncertainty estimates than the ones of the local flow quantities.

4.1.2 Spalart & Allmaras model

The convergence of the local flow quantities at the three selected locations is presented in figure 3. With this model, we have solutions with the two discretization techniques. As expected, the results obtained with the FD and FV versions of PARNASSOS are consistent.

In general, the FV version shows a smaller sensitivity to the grid set selected than the FD discretization. Bearing in mind that the FD version discretizes the equations in Contravariant form, this result is not surprising.

The behaviour of the pressure coefficient at $x = 5.357h, 0.107h$ is a good example of the difficulties of making uncertainty estimations when the data do not change monotonically. The uncertainty estimation performed for the 201×201 grid of set B is completely in disagreement with the rest of the data obtained for this location.

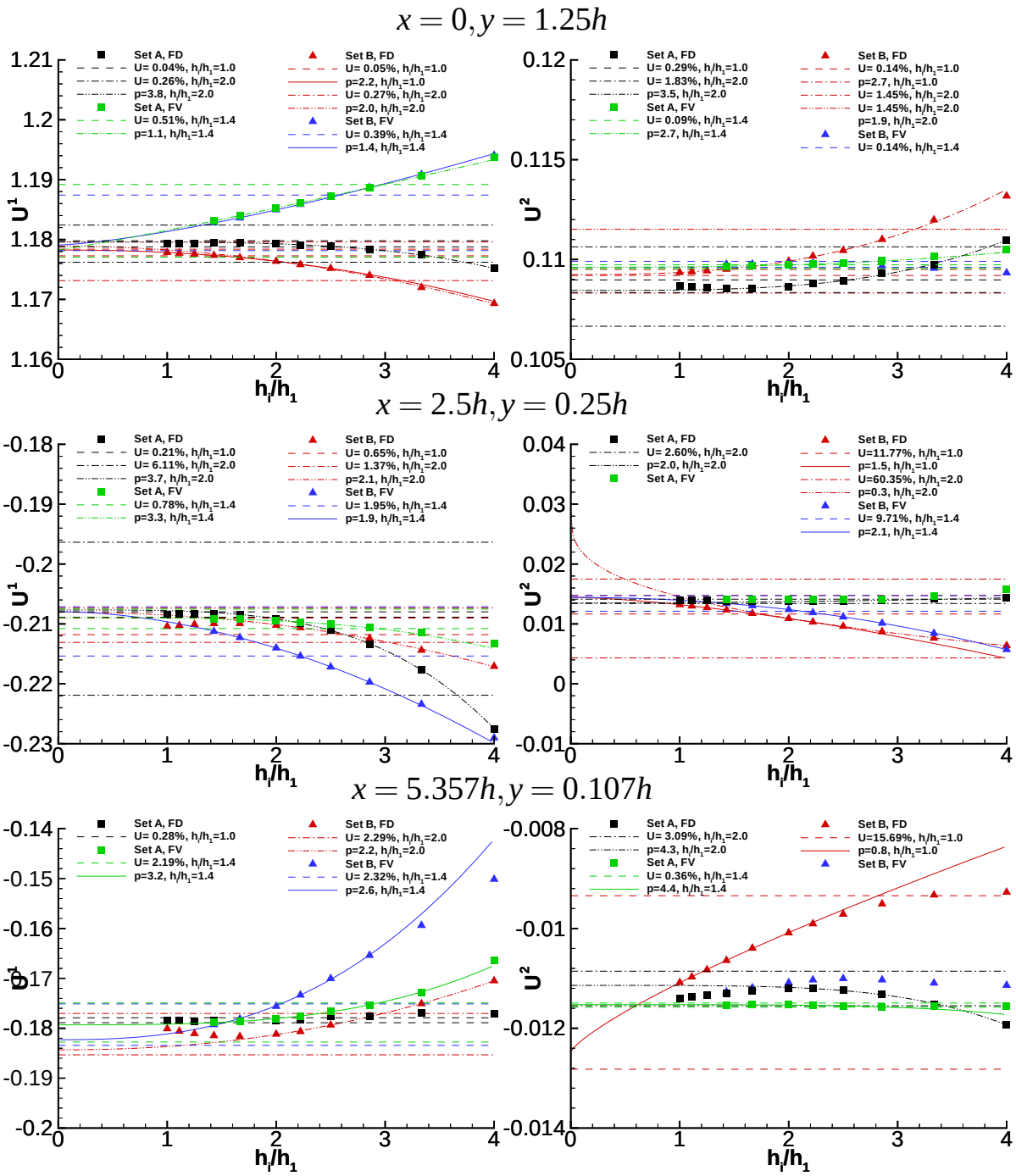

Figure 3: Convergence with the grid refinement of local flow quantities. Flow over a 2-D hill calculated with Spalart & Allmaras one-equation model.

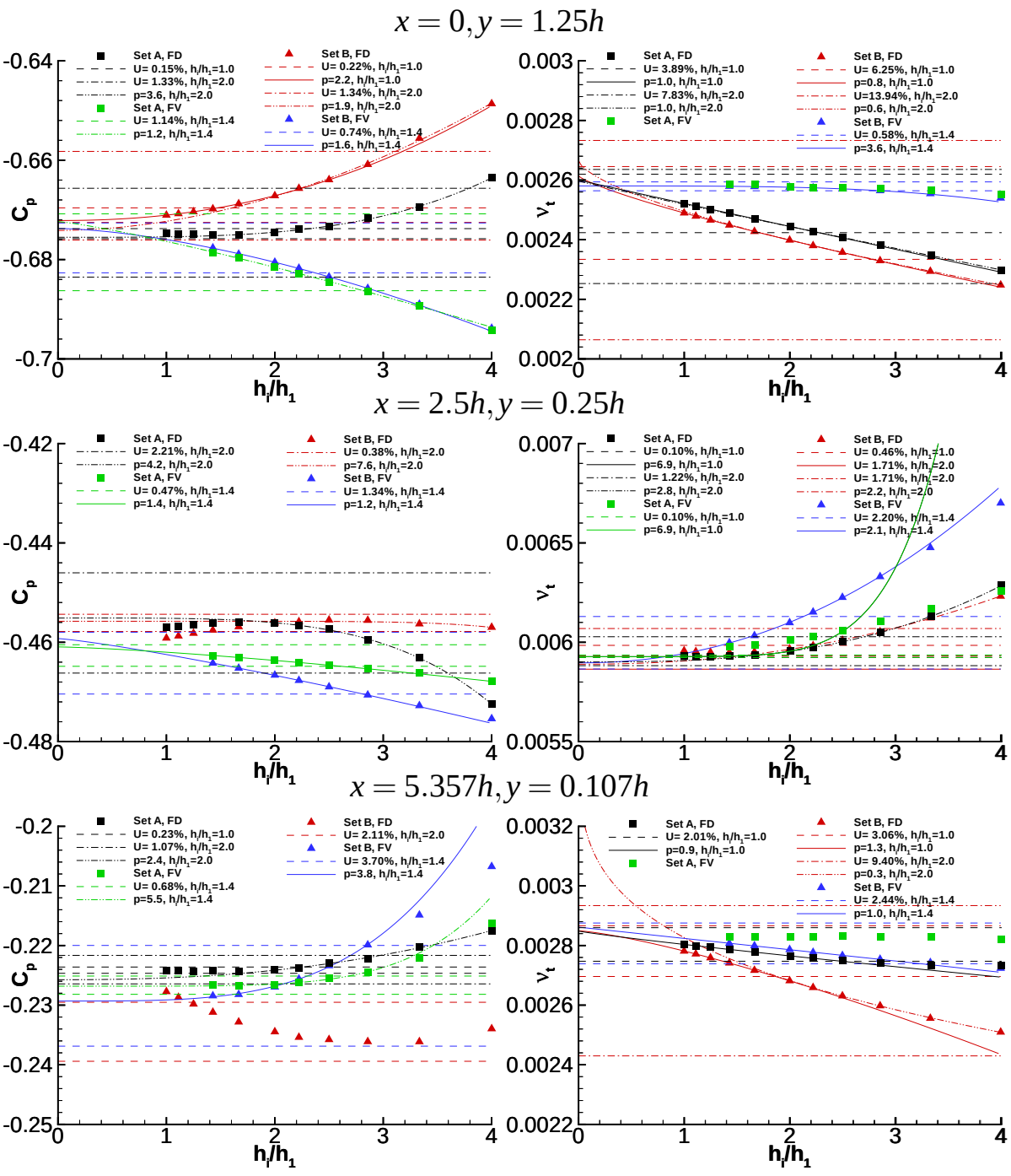

Figure 3: (Cont.) Convergence with the grid refinement of local flow quantities. Flow over a 2-D hill calculated with Spalart & Allmaras one-equation model.

The convergence of the separation and re-attachment points with the grid refinement is illustrated in figure 4. The same figure shows the three resistance coefficients as a function of the grid density.

The uncertainty is larger for the FV results than for the FD version. However, the FV approach shows again a remarkable insensitivity to the grid set selected.

The results and respective error bars of the various calculations are all consistent. The uncertainty of the friction resistance coefficient of the FV calculations is larger than the one obtained for the FD

version.

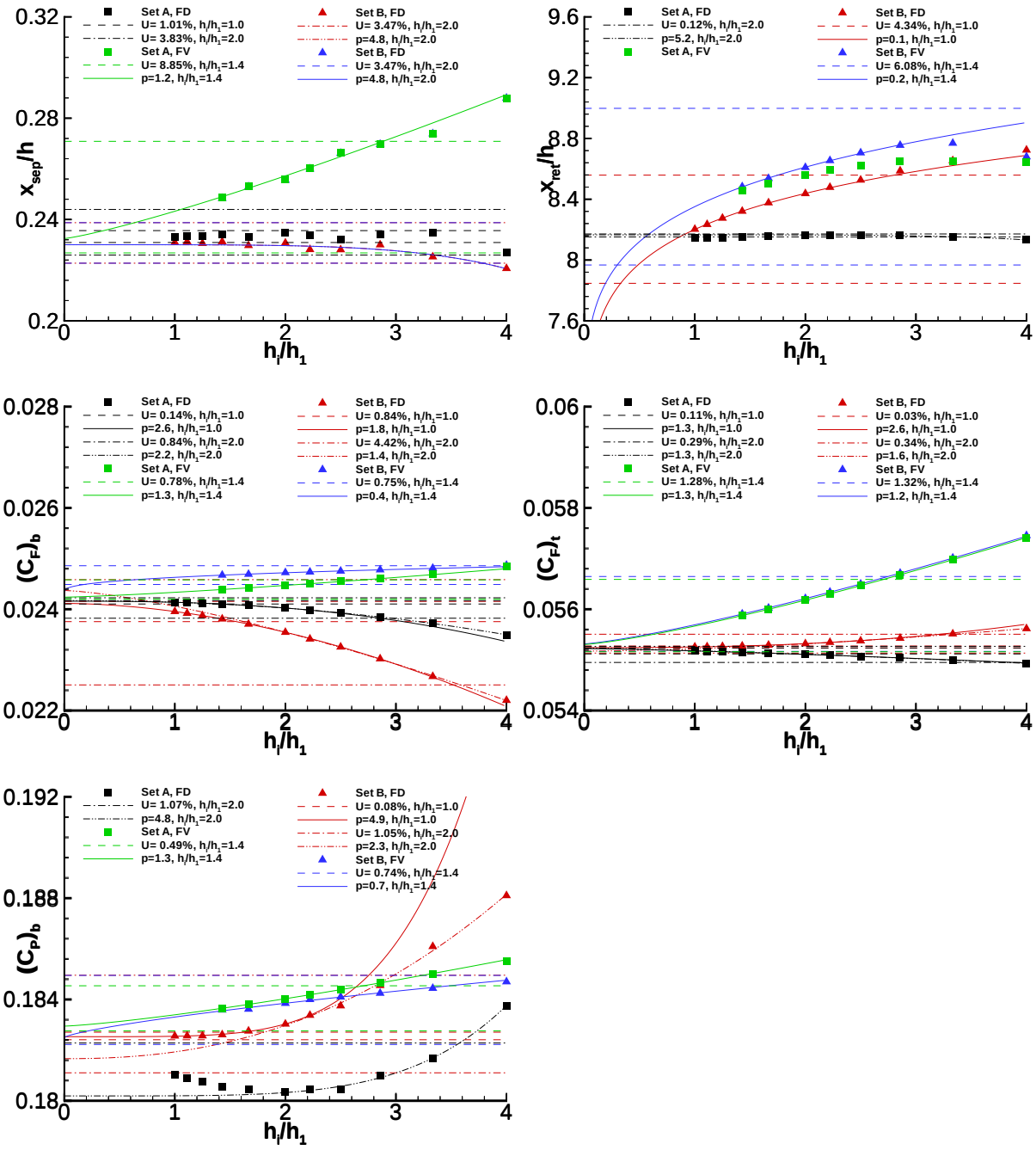

Figure 4: Convergence with the grid refinement of separation and re-attachment points and resistance coefficients. Flow over a 2-D hill calculated with Spalart & Allmaras one-equation model.

4.2 Flow over a backward facing step, case C-30

For this test case there are three sets of 7 grids. The uncertainties are estimated for the finest grid of 241×241 nodes using the data of the 6 finest grids, which cover a grid refinement ratio of 2.

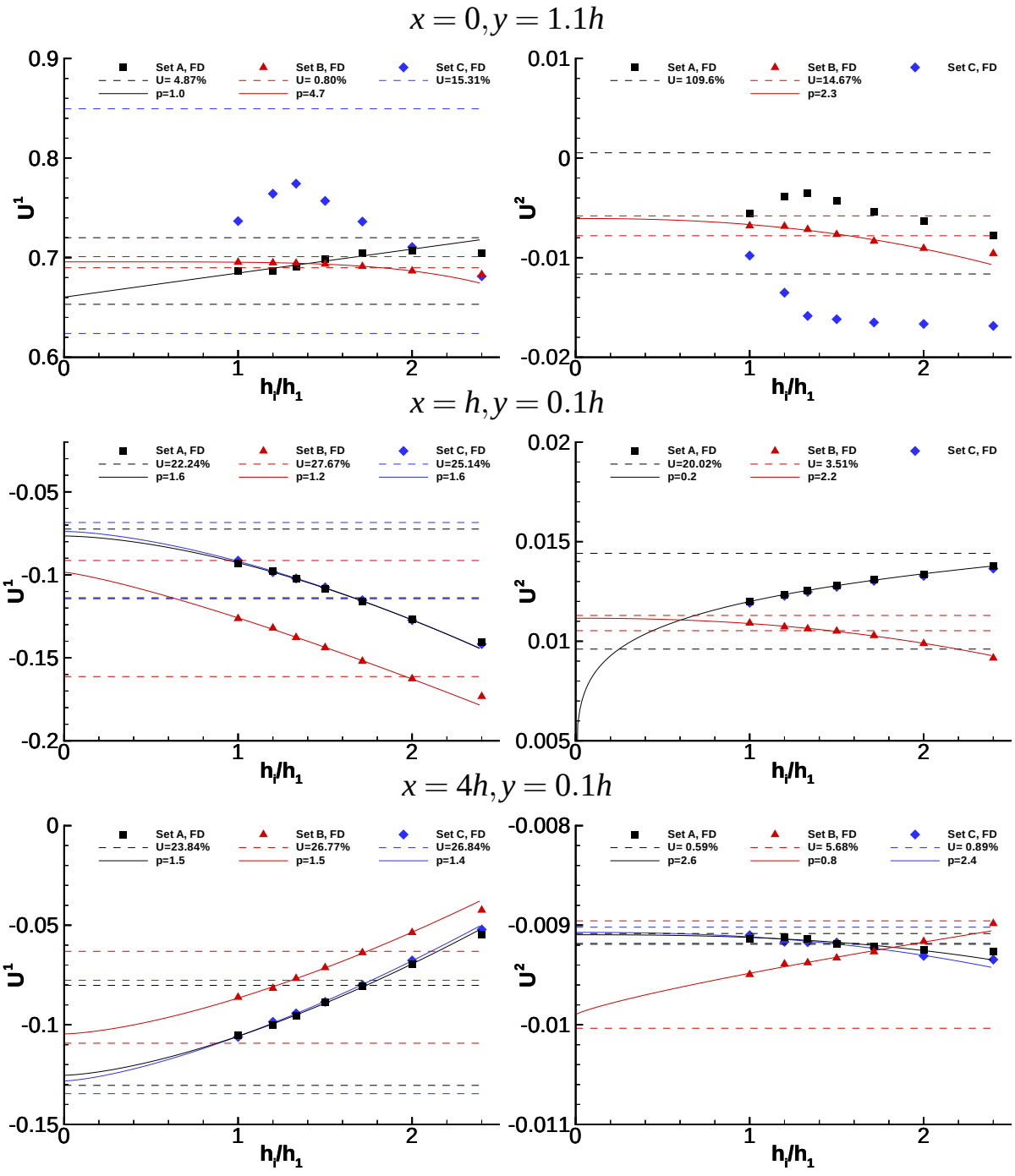

Figure 5: Convergence with the grid refinement of local flow quantities. Flow over a backward facing step calculated with Menter's one-equation model.

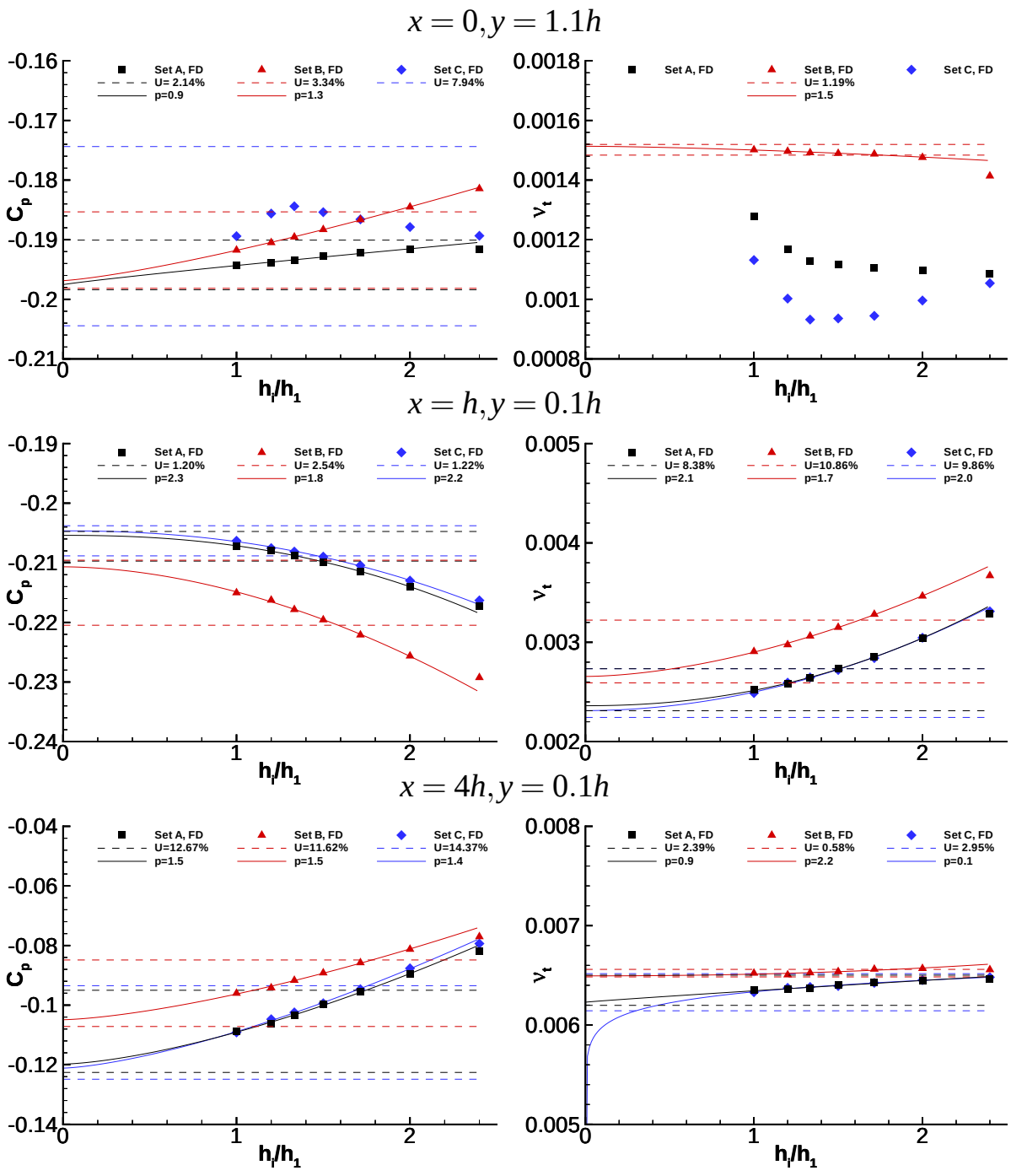

Figure 5: (Cont.) Convergence with the grid refinement of local flow quantities. Flow over a backward facing step calculated with Menter's one-equation model.

4.2.1 Menter's model

With this turbulence model we have only applied the FD version to the three grid sets available. The convergence of the local flow quantities is illustrated in figure 5. The data obtained for the three

grid sets suggest the following remarks:

- Close to the top corner of the step, the results of grid set C have clearly more difficulty to converge than the other two grid sets. This is not unexpected due to the absence of a grid node at the corner for this grid set.
- In the other two locations, the behaviour on the "Cartesian" grid is distinct from that on the other two sets which are perfectly equivalent. Nevertheless, there is overlap between the estimated error bars.

Figure 6 presents the convergence behaviour of the re-attachment point and of the resistance coefficients at the two walls. The best agreement between the three grid sets is obtained for the friction resistance at the top wall. The pressure resistance coefficient obtained in set B and its respective error bar does not intersect the results of the other two grid sets. The pressure at the wall is determined with the solution of the momentum equation in the normal direction using backward or forward differencing; so the lack of orthogonality at the boundary of the grids of set B is probably responsible for this result.

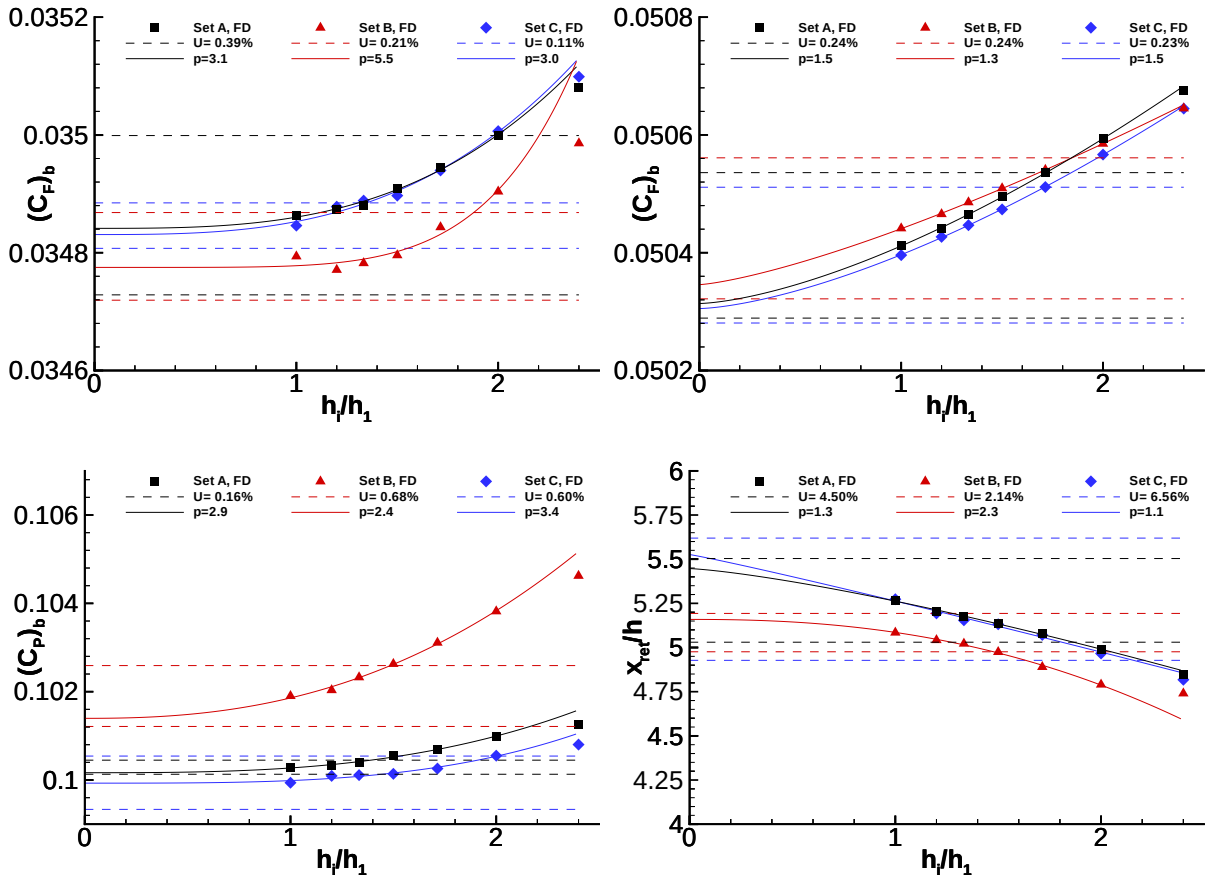

Figure 6: Convergence with the grid refinement of re-attachment point and resistance coefficients. Flow over a backward facing step calculated with Menter's one-equation model.

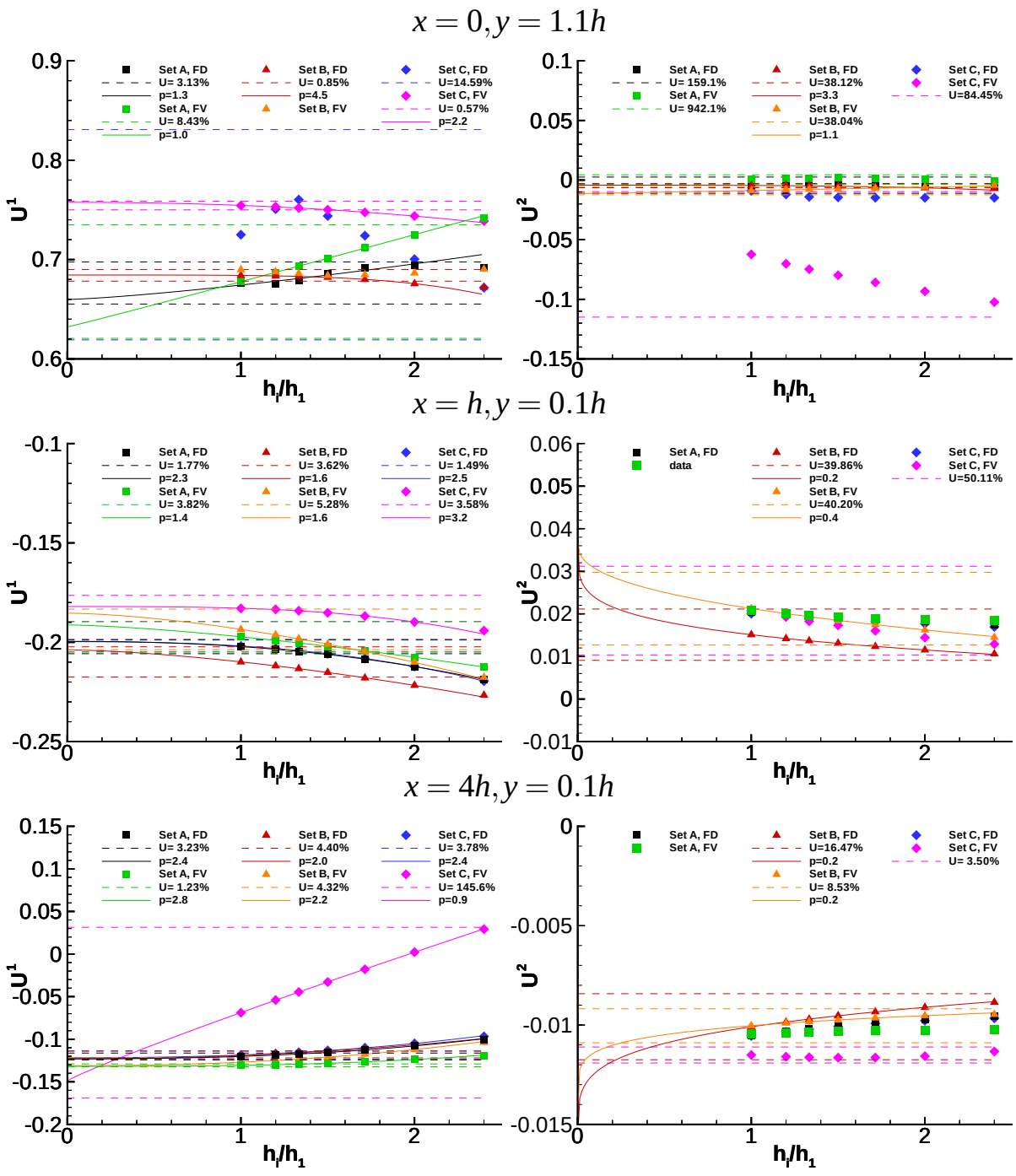

Figure 7: Convergence with the grid refinement of local flow quantities. Flow over a backward facing step calculated with Spalart & Allmaras one-equation model.

4.2.2 Spalart & Allmaras model

With the Spalart & Allmaras turbulence model we have performed calculations with the two versions of PARNASSOS. The convergence of the local flow quantities with the grid refinement is pre-

sented in figure 7. There are several interesting features in the data:

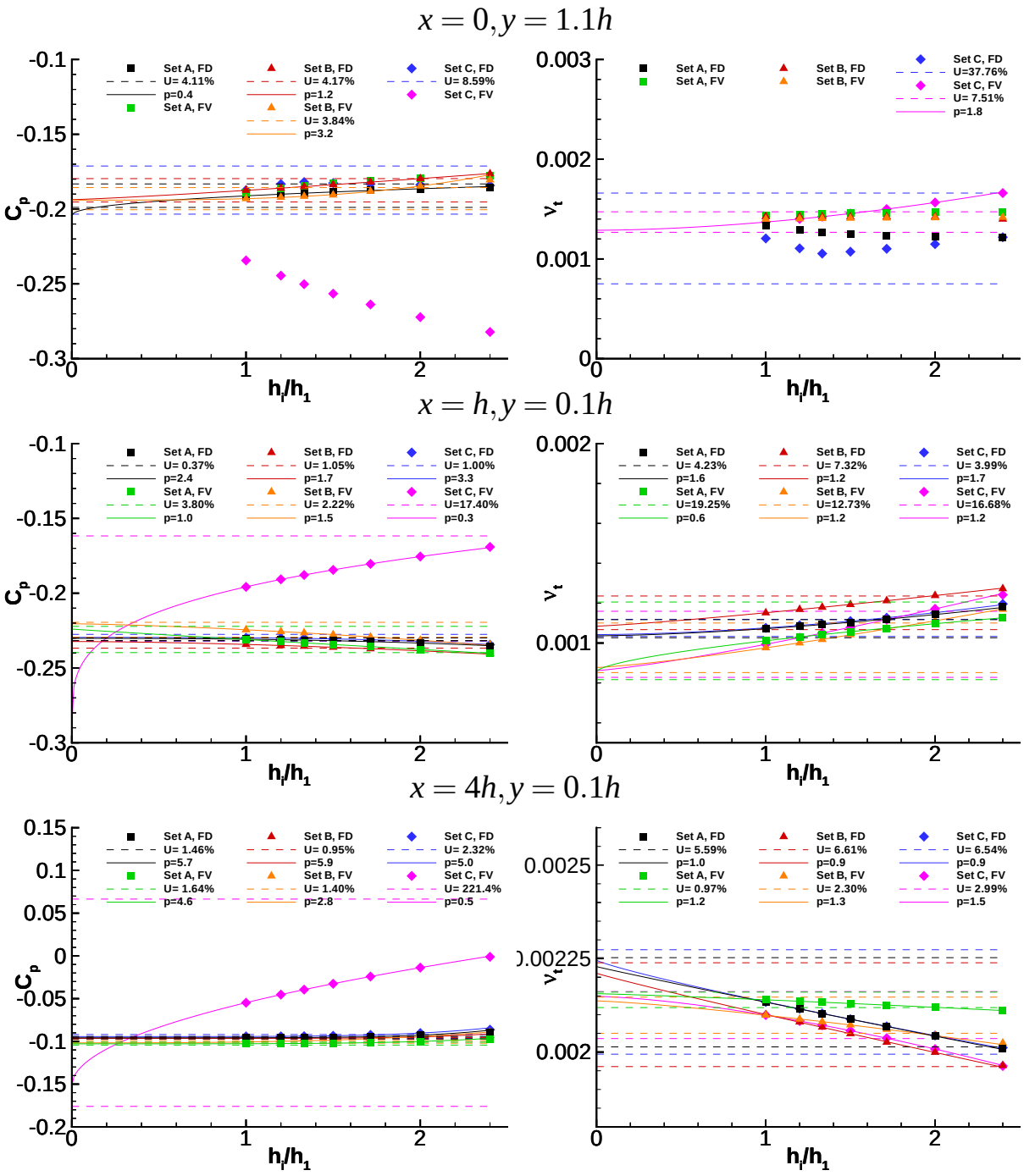

Figure 7: (Cont.) Convergence with the grid refinement of local flow quantities. Flow over a backward facing step calculated with Spalart & Allmaras one-equation model.

- Close to the top corner of the step, the results of grid set C exhibit anomalous convergence. This is particularly evident for the FV results for U^2 and C_p. The FD difference approach is less sensitive to the absence of a grid node at the corner of the step.

- C_p from the FV method close to the lower corner of the step converges much slower than in the solutions on other grids. However, a similar effect is not present in the other flow variables at the same location.

- A more puzzling result is the behaviour of the FV U^1 and C_p close to re-attachment. The grid set C results exhibit a much larger grid dependency than all the other solutions. On the other hand, the FV and FD versions lead to very similar results on grid sets A and C.

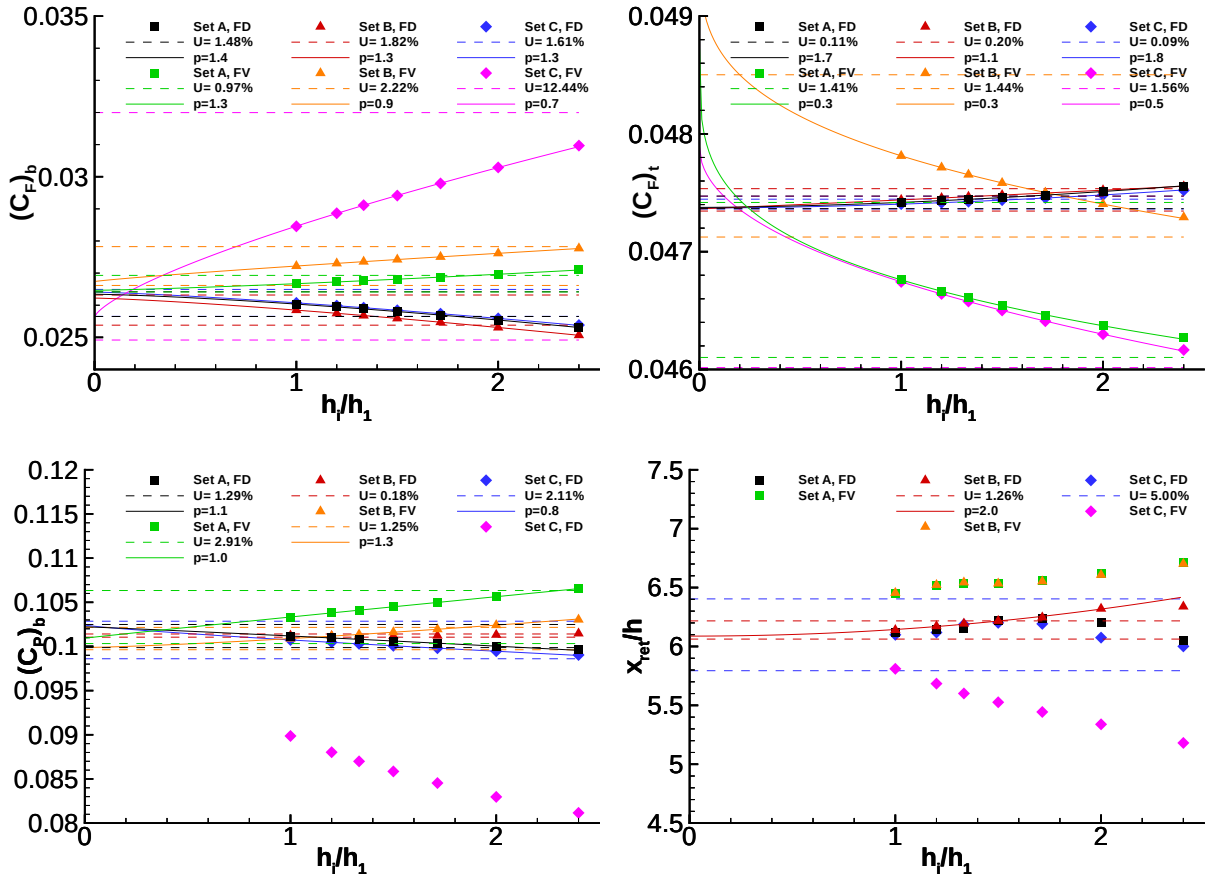

Figure 8: Convergence with the grid refinement of re-attachment points and resistance coefficients . Flow over a backward facing step calculated with Spalart & Allmaras one-equation model.

The re-attachment point and resistance coefficients are plotted in figure 8 as a function of the grid refinement. The values of x_{ret} of the FV solution of grid set C exhibit again the largest dependency on the grid refinement level.

The results of the friction resistance coefficient at the bottom boundary are encouraging. All the error bars overlap and there is an excellent agreement between the FD and FV methods. Once more, the largest uncertainty is estimated for the FV solution in set C.

The friction resistance coefficient at the top wall obtained with the FV version exhibits an awkward behaviour. In this case, the results of grid sets A and C are very similar, but grid set B leads to larger values of $(C_F)_b$. This behaviour of the data is a consequence of the determination of the distance to

the wall in the FV version, which in a non-orthogonal grid will not be very accurate. On the other hand, the FV version leads to very small uncertainties and perfectly consistent results in the three grid sets.

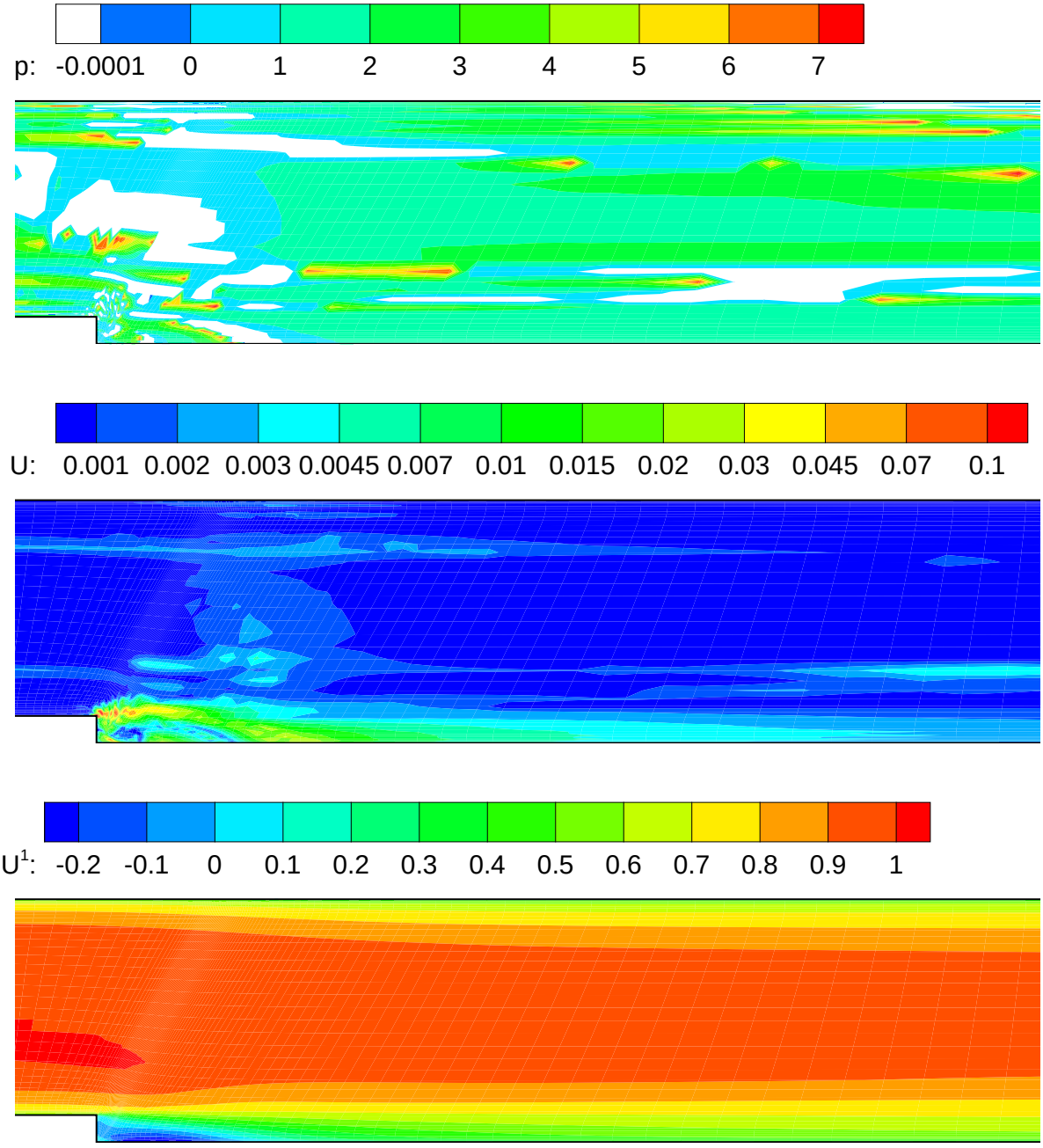

Figure 9: U^1 field with its estimated uncertainty and observed order of accuracy. Flow over a backward facing step calculated with Spalart & Allmaras one-equation model and FD version of PARNASSOS.

The behaviour of the pressure resistance coefficient of the FV results on grid set C must be at-

tributed to the absence of grid nodes at the corners of the step.

As an example of an uncertainty estimation for the complete flow field, we have have applied our procedure to estimate the uncertainty in U^1 on the finest grid FD solution of set A for those 101x101 points which appear in all grids. Figure 9 presents the contour maps of U^1, the estimated uncertainty, U, and the observed order of accuracy p.

As expected, the region of maximum uncertainty is close to the two corners of the step, specially the top corner. The observed order of accuracy is close to its theoretical value for most of the field. However, there are several locations where it reaches completely unreasonable values.

The white regions in the plot of p correspond to the locations where it is not possible to determine convergence conditions, whether monotonic or oscillatory. It is clear that there are several of these locations where the differences between the numerical solutions are small, because the estimated uncertainty based on the maximum difference between the solutions leads to low uncertainties. This result suggest that the present approach of "ignoring" apparent divergence is a viable approach if carefully interpreted.

5 Conclusions

The finite-differences and finite-volume versions of PARNASSOS have been applied to the five grid sets available for the Workshop on CFD Uncertainty Analysis. The one-equation model proposed by Menter has been applied with the finite-differences code whereas the Spalart & Allmaras model has been applied with both versions.

Uncertainty estimations have been made for the selected flow quantities using a least squares root version of the Grid Convergence Index method.

As one could expect, the solutions obtained with the two versions of PARNASSOS are similar, but the convergence properties of the two discretization techniques are not identical. In particular, the absence of grid nodes at the corners of the step has a much stronger effect on the finite volume version than on the finite-differences code.

The results obtained with the present verification procedure our encouraging. However, a wide range of observed orders of accuracy is obtained and there are several situations where it is difficult to classify the convergence condition. Therefore, the application of the present procedure to practical calculations still requires some experience and careful interpretation to obtain a reliable uncertainty estimation based on Richardson extrapolation.

References

[1] Roache P.J. - *Verification and Validation in Computational Science and Engineering* - Hermosa Publishers, 1998.

[2] Eça L, Hoekstra M. - *On The Grid Sensitivity Of The Wall Boundary Condition Of The $K-\Omega$ Turbulence Model*- Accepted for publication in the Journal of Fluids Engineering, 2004.

[3] Eça L, Hoekstra M. - *An Evaluation of Verification Procedures for CFD Applications* - 24^{th} Symposium on Naval Hydrodynamics, Fukuoka, Japan, July 2002.

[4] Eça L., Hoekstra M. - *A Verification Exercise for Two 2-D Steady Incompressible Turbulent Flows* - IV European Congress on Computational Methods In Applied Sciences And Engineering, ECCOMAS 2004, July 2004.

[5] Proceedings of the Workshop on CFD Uncertainty Analysis - Eça L, Hoekstra M. Eds., Lisbon, October 2004.

[6] José M.Q.B. Jacob, Eça L. - *2-D Incompressible Steady Flow Calculations with a Fully Coupled Method* - VI Congresso Nacional de Mecnica Aplicada e Computacional, Aveiro, April 2000

[7] Hoekstra M. - *Numerical Simulation of Ship Stern Flows with a Space-marching Navier-Stokes Method* - PhD Thesis, Delft 1999.

[8] Spalart P.R., Allmaras S.R. - *A One-Equations Turbulence Model for Aerodynamic Flows* - AIAA 30th Aerospace Sciences Meeting, Reno, January 1992.

[9] Menter F.R. - *Eddy Viscosity Transport Equations and Their Relation to the $k-\varepsilon$ Model* - Journal of Fluids Engineering, Vol. 119, December 1997, pp. 876-884.

[10] Saad Y, Schultz M.H. - *GMRES: a generalized minumum residual algorithm for solving non-symmetric linear systems* - SIAM Jnl. Sci. Statist. Comp., Vol. 7, pp 856-869, 1986.